

RESEARCH

Open Access



The TEAD4-DYNLL1 axis accelerates cell cycle progression and augments malignant properties of lung adenocarcinoma cells

Dapeng Li^{1†}, An Wang^{2†}, Xuan Wang^{2†}, Mengkun Shi², Xiaofeng Chen², Yubao Lyu^{3*} and Dayu Huang^{2*}

Abstract

Background Lung adenocarcinoma (LUAD) is a major contributor to global mortality. Grounded onto bioinformatics insights, this study probes the functions of dynein light chain LC8-type 1 (DYNLL1) in LUAD progression.

Methods DYNLL1 levels in LUAD and normal cells were determined using qPCR and western blotting analyses. Lentiviral plasmids-mediated DYNLL1 silencing was induced in LUAD cells, followed by functional assays to investigate DYNLL1's impacts on proliferation, mobility, apoptosis, and cell cycle distribution. KY19382, a Wnt/ β -catenin agonist, was employed to analyze the involvement of the Wnt/ β -catenin pathway in DYNLL1's effects. Upstream regulator of DYNLL1 was queried using bioinformatics. Mouse LUAD cells LA795 were implanted into BALB/c nude mice to establish animal tumor models.

Results DYNLL1 exhibited heightened expression in LUAD cells. Its artificial silencing reduced proliferation and dissemination of cancer cells, promoted cell apoptosis, and induced G0/G1 cell cycle arrest. DYNLL1 silencing reduced β -catenin levels in cancer cells, and KY19382 treatment diminished the effects induced by DYNLL1 silencing. TEA domain transcription factor 4 (TEAD4), upregulated in LUAD cells, binds to the DYNLL1 promoter for transcriptional activation. TEAD4 silencing in LUAD cells reduced DYNLL1 transcription and β -catenin levels, thus suppressing proliferation while promoting apoptosis, senescence, and cell cycle arrest. In vivo, TEAD4 silencing weakened tumorigenesis of LA795 cells. Nevertheless, these phenomena were counteracted by the artificial DYNLL1 restoration in LUAD cells.

Conclusion This investigation demonstrates a TEAD4-DYNLL1 axis that accelerates cell cycle progression and augments malignant properties of LUAD cells via the Wnt/ β -catenin pathway.

Keywords Lung adenocarcinoma, TEAD4, DYNLL1, Cell cycle, Wnt/ β -catenin pathway

[†]Dapeng Li, An Wang, and Xuan Wang contributed equally to this work.

*Correspondence:

Yubao Lyu

411245033@qq.com

Dayu Huang

huangdayu@huashan.org.cn

¹ Department of Oncology, The First Affiliated Hospital of Soochow University, Suzhou 215006, Jiangsu, People's Republic of China

² Department of Thoracic Surgery, Huashan Hospital of Fudan University, Shanghai 200040, People's Republic of China

³ Department of Integrative Medicine, Huashan Hospital of Fudan University, Shanghai 200040, People's Republic of China

Introduction

Lung cancer ranks as the most prevalent and lethal malignant tumor in China and globally, with lung adenocarcinoma (LUAD) representing the predominant form, constituting about 40% of all lung cancer diagnoses [1]. Currently, treatment strategies for LUAD have evolved from conventional methods such as surgery, radiation, and chemotherapy to more personalized and precise approaches, including targeted therapies [2]. For instance, mutations in the epidermal growth factor receptor gene are identified in nearly 50% of LUAD



cases. This has contributed to the development of tyrosine kinase inhibitors, which have been shown to markedly enhance patient outcomes [3, 4]. Despite continual advancements in therapeutic strategies, the overall survival rate for LUAD patients remains dishearteningly low [2, 5]. The primary reason for this is that a majority of patients receive their diagnoses at advanced stages, limiting their chances for effective interventions [6]. Alarming, some patients may succumb to recurrent lung cancer even when diagnosed early and provided with optimal treatments [7, 8]. Thus, developing drugs that aim at other pathogenic genes could represent a viable strategy moving forward.

In our research, we conducted bioinformatics analyses, identifying dynein light chain LC8-type 1 (DYNLL1) as a promising prognostic biomarker for LUAD. The LC8 light chains act as central proteins that form homodimers, featuring dynamic binding grooves that interact with numerous proteins and participate in various cellular functions, including mitosis, microtubule stabilization, intracellular transport, postsynaptic density organization, nuclear transport, apoptosis, and transcription regulation [9–11]. DYNLL1 plays a key role in regulating mitosis, especially in spindle assembly and chromosome distribution [12]. Importantly, DYNLL1 has emerged as a potential oncogene in various human cancers. Research has indicated its capacity to hasten cell cycle progression in hepatocellular carcinoma and contribute to resistance against chemotherapy [13]. Moreover, DYNLL1 has been implicated in facilitating the hepatocellular carcinoma progression by activating the Wnt/ β -catenin pathway [14]. The canonical Wnt pathway operates by stabilizing β -catenin via Dishevelled-mediated mechanisms. This stabilization allows β -catenin to act as a transcriptional co-activator, leading to increased cell cycle progression, proliferation, differentiation, and overall growth, in addition to promoting cellular migration and influencing embryonic development processes [15]. Up until this point in our research, the specific role of DYNLL1 in LUAD remains unclear. We hypothesized that a similar DYNLL1-Wnt/ β -catenin interplay could be significant in mediating cell cycle dynamics and the malignant transformation associated with DYNLL1 in LUAD.

Further bioinformatics analyses pointed to TEA domain transcription factor 4 (TEAD4) as a potential key regulatory factor for DYNLL1. TEAD4 is recognized as an essential member of the TEAD family, known for its involvement in promoting cell survival, enhancing proliferation, and contributing to therapeutic resistance in various cancer types [16]. Given these insights, our study was designed to investigate the interaction between TEAD4 and DYNLL1, along with their respective biological roles in LUAD progression.

Methods

Cells

Human bronchial epithelial cells BEAS-2B (BNCC359274) were purchased from BeNa Culture Collection (Beijing, China) and maintained in DMEM-H (BNCC364169, BeNa). Human LUAD cell lines A549 (CL-0016), NCI-H1395 (CL-0275), and NCI-H441 (CL-0514), and mouse LUAD cell line LA795 (CL-0376) were obtained from Procell Life Science & Technology (Wuhan, Hubei, China). A549 cells were maintained in Ham's F-12K medium, while NCI-H1395, NCI-H441, and LA795 cells were maintained in RPMI-1640. All media were filled with 10% FBS and 1% antibiotics. The culture conditions were maintained at 37 °C with 5% CO₂.

Cell transfection and treatment

NCI-H1395, NCI-H441, and LA795 cells were plated into 96-well plates. Lentiviral vectors for knockdown of TEAD4 (KD-TEAD4), knockdown of DYNLL1 (KD-DYNLL1), and overexpression of DYNLL1 (OE-DYNLL1) were obtained from VectorBuilder Inc. (Guangzhou, Guangdong, China). Cells were infected with the lentiviral vectors for 24 h, followed by medium replacement. Puromycin (10 μ g/mL) was used to select transfected cells for 1 week to obtain stably transfected cell lines. KY19382 (1 μ M, HY-131447, MedChemExpress [MCE], Monmouth Junction, NJ, USA), a Wnt/ β -catenin agonist, was utilized to treat the stable transfected cells for 24 h before conducting subsequent assays [17].

RNA isolation and quantification

After isolating total RNA utilizing the TRIzol reagent (15596018CN, Thermo Fisher Scientific, Rockford, IL, USA), cDNA was synthesized using ABScript Neo RT Master Mix for qPCR (RK20432, Abclonal Biotechnology Co., Ltd., Wuhan, Hubei, China). Afterward, qPCR analysis was conducted on an ABI QuantStudio 5 Real-Time PCR System (A28569, Thermo Fisher Scientific, Rockford, IL, USA) utilizing Genious 2X SYBR Green Fast qPCR Mix (RK21204, Abclonal). With GAPDH served as an endogenous reference, quantitative analysis was conducted using the 2^{- $\Delta\Delta$ CT} method. The primer sequences (all 5'–3') used included: TEAD4 (F) GAA GGTCTGCTCTTTCGGCAAG, TEAD4 (R) GAGGTG CTTGAGCTTGTGGATG; DYNLL1 (F) GCTACTCAG GCGCTGGAGAAAT, DYNLL1 (R) GTGTCACATAAC TACCGAAGTTC; GAPDH (F) GTCTCCTCTGAC TTCAACAGCG, GAPDH (R) ACCACCCTGTTGCTG TAGCCAA.

Colony formation assays

NCI-H1395 and NCI-H441 cells were digested and resuspended in RIPA-1640, counted, and approximately

1000 cells per well were plated into 6-well plates. The cells were cultured in standard conditions for 2 weeks with the media refreshed once every 3 days. After culture, the cells were fixed, followed by staining with 0.1% crystal violet for 20 min. Colonies with no less than 50 cells were enumerated under an optical microscope (X43, Olympus Optical Co., Ltd, Tokyo, Japan).

Wound healing assays

NCI-H1395 and NCI-H441 cells were plated into 6-well plates until confluence. A 200 μ L pipette tip was utilized to create scratches. After washing with PBS (pH 7.4) to discard cell debris, images were captured. After incubation in serum-free medium at 37 °C for 24 h, images of wound healing were taken at 0 and 24 h using the optical microscope (X43, Olympus). The wound healing rate was calculated as: $100\% \times (\text{wound width}_{0\text{h}} - \text{wound width}_{24\text{h}}) / \text{wound width}_{0\text{h}}$ to evaluate cell migration within 24 h.

Transwell assays

NCI-H1395 and NCI-H441 cells were collected, starved overnight, and plated into the apical wells of Transwell inserts pre-coated with Matrigel. Complete medium filled with 20% FBS (800 μ L) was loaded to the basolateral wells. After 24 h, cells that invaded the basolateral wells were fixed and underwent crystal violet staining. The number of invasive cells was enumerated under the microscope (X43, Olympus), and the 24-h invasion rate was calculated.

Apoptosis and cell cycle analysis

Apoptosis was analyzed following the guidelines of the Annexin V-FITC/PI kit (HY-K1073, MCE). Briefly, treated NCI-H1395 and NCI-H441 cells were harvested, washed, resuspended, and subjected to Annexin V-FITC and PI staining. After incubation for 20 min in the dark, apoptosis was analyzed utilizing a flow cytometer (FACS Canto, BD Biosciences, San Jose, CA, USA). To analyze cell cycle distribution, the cells were fixed with 70% ethanol for 30 min, followed by PI staining for 30 min. The cell cycle distribution was then analyzed on the FACS Canto flow cytometer.

SA- β -Gal (SABG) staining

Treated NCI-H1395 and NCI-H441 cells were harvested and fixed in β -Gal fixative (G1580, Solarbio Science & Technology Co., Ltd., Beijing, China) at room temperature for 15 min. Subsequently, cells underwent PBS washes and overnight incubation at 37 °C in staining solution. Cells with positive staining were enumerated under the microscope (X43, Olympus), and the positive cell rate was calculated.

Immunofluorescence staining

After fixing, the NCI-H1395 and NCI-H441 cells underwent permeabilization with 0.3% Triton X-100 and blocking with 10% goat serum for 2 h. Ki67 primary antibody (1:100, GTX20833, GeneTex Inc., San Antonio, TX, USA) was applied for overnight incubation at 4 °C. Subsequently, the cells were probed with goat anti-rabbit IgG H&L (Alexa Fluor® 647) (1:200, ab150079, Abcam Inc., Cambridge, MA, USA) for 2 h in the dark. After nuclear staining using DAPI, images were taken under a fluorescence microscope (Leica DMI8, Leica Microsystems, Solms, Germany), and fluorescence intensity was quantified using Image J (version 1.53, National Institutes of Health, USA).

Chromatin immunoprecipitation (ChIP)-qPCR

NCI-H1395 and NCI-H441 cells were harvested and crosslinked with 1% formaldehyde for 10 min at room temperature to capture protein-DNA interactions. The reaction was quenched by adding glycine to a final concentration of 125 mM for 5 min. Chromatin was fragmented by sonication using a Bioruptor (Diagenode, Belgium) to achieve an average fragment size of 200–500 bp. Cell lysates were prepared and incubated with TEAD4 antibody (1:30, ab308621, Abcam) overnight at 4 °C for immunoprecipitation. Rabbit IgG (1:30, ab172730, Abcam) served as a negative control. After incubation, protein-DNA complexes were captured using magnetic beads (Dynabeads Protein A, Thermo Fisher). The beads were washed to remove nonspecific bindings and then eluted. To reverse crosslinking, samples were heated at 65 °C overnight, followed by protein digestion with proteinase K (Roche Ltd, Basel, Switzerland). DNA was purified using a QIAquick PCR purification kit (Qiagen GmbH, Hilden, Germany). Following this, qPCR analysis was conducted using primers designed for the DYNLL1 promoter sequences.

Luciferase assays

The DYNLL1 promoter was amplified and inserted into the pGL3-basic vector (E1751, Promega Corporation, Madison, WI, USA). The reporter vector was co-transfected with the KD-TEAD4 into NCI-H1395 and NCI-H441 cells utilizing Lipofectamine 3000 (L3000150, Thermo Fisher). After 48 h, luciferase activity was determined following the protocols of the dual-luciferase reporter assay system (E1910, Promega).

Animal models

Female BALB/c nude mice (3–4 weeks old, 16–20 g) were provided by Anburui Biotechnology Co., Ltd. (Fujian, China) and used in guidelines approved by the

Institutional Animal Care and Use Committee of the First Affiliated Hospital of Soochow University (approval no. 2024-HSYY-551). To establish the allograft tumor model, LA795 cells (5×10^6) stably transfected with KD-TEAD4, OE-DYNLL1 were injected into the mice subcutaneously. These procedures resulted in four groups: KD-NC, KD-TEAD4, KD-TEAD4+OE-NC, and KD-TEAD4+OE-DYNLL1, with six mice per group. The length and width of tumors were measured every 7 days using calipers, and tumor growth was assessed by volume calculation ($V = L \times W^2 / 2$). After 35 days, the mice were euthanized with 150 mg/kg nembutal, and the tumors were excised and weighed, followed by paraffin embedding for subsequent experiments.

Immunohistochemistry (IHC)

Prepared tumor tissue Sects. (4 μm thick) were deparaffinized with xylene and dehydrated in ethanol. The sections were incubated in 3% H_2O_2 and blocked with 10% (v/v) BSA (A8010, Solarbio) for 2 h. Primary antibodies for Ki67 (1:100, GTX20833, GeneTex), PCNA (1:100, GTX100539, GeneTex), Cyclin D1 (1:100, ab16663, Abcam), and P21 (1:500, MA5-31479, Thermo Fisher) were applied overnight. HRP-goat anti-mouse (1:500, G-21040, Thermo Fisher) or HRP-goat anti-rabbit (1:200, G-21234, Thermo Fisher) secondary antibodies were added, followed by DAB staining. After counterstaining with hematoxylin, the positive cell rate was quantified.

Terminal deoxynucleotidyl transferase (TdT)-mediated dUTP nick end labeling (TUNEL) assays

All procedures were performed according to the instructions provided with the Biotin TUNEL Apoptosis Assay Kit (T2191, Solarbio). After deparaffinization and rehydration, the allograft tumor tissue sections were incubated with proteinase K for 10 min to facilitate permeabilization. Following washing with PBS, the sections were treated with 3% hydrogen peroxide (H_2O_2) for [insert duration here, e.g., 10 min] to block endogenous peroxidase activity. The TUNEL reaction solution was then applied and incubated in the dark at 37 °C for 1 h. After washing with PBS, Streptavidin-HRP was applied and incubated at 37 °C for 30 min. DAB (DA1010, Solarbio) was used for visualization, and the nuclei were counterstained with hematoxylin. The TUNEL-positive rate was then calculated.

Western blotting (WB) analysis

Cells and tumor tissues were lysed with RIPA buffer (89901) for total protein extraction. Equal amounts of protein samples underwent 10% SDS-PAGE separation and were loaded onto PVDF membranes. Following blocking with 5% skim milk, these membranes were

probed with antibodies for DYNLL1 (1:1000, ab51603, Abcam), Cyclin D1 (1:200, ab16663, Abcam), P21 (1:1000, MA5-31479, Thermo Fisher), β -catenin (1:100, A11512, Abclonal), TEAD4 (1:1000, 12418-1-AP, Proteintech Group, Wuhan, Hubei, China), GAPDH (1:5000, 10494-1-AP, Proteintech) overnight. This was followed by incubation with HRP-conjugated goat anti-mouse (1:5000, G-21040, Thermo Fisher) or goat anti-rabbit (1:5000, G-21234, Thermo Fisher) IgG. Following this, protein bands were visualized by enhanced chemiluminescence, and band intensity was analyzed utilizing Image J (version 1.53, National Institutes of Health, USA).

Statistical analysis

Data were analyzed using Prism 10.0 software (GraphPad, La Jolla, CA, USA). Data were obtained from a minimum of three independent replicates and are exhibited as the mean \pm SEM. Statistical differences were assessed using one-way or two-way ANOVA, followed by Tukey's multiple comparisons test. A p value < 0.05 was deemed statistically significant.

Results

DYNLL1 is abnormally upregulated in LUAD

To identify candidate prognostic biomarkers or treatment targets for LUAD, the top 100 Most Differential Survival Genes in LUAD were downloaded from the GEPIA database (<http://gepia.cancer-pku.cn/index.html>), and the top 100 Prognostic Markers in LUAD were obtained from the UALCAN database (<http://ualcan.path.uab.edu/index.html>). The intersection of these two sets of genes revealed 14 shared genes (Fig. 1A). A protein-protein interaction (PPI) network for the intersecting genes was generated, which highlighted a central interacting protein network consisting of ANLN, PLK1, DYNLL1, CCNB1, and TACC3 (Fig. 1B). Notably, DYNLL1 stands out as the only gene within this group whose functional roles in LUAD remain to be fully characterized. Existing research indicates that DYNLL1 could potentially expedite cell cycle progression [13] and promote tumorigenesis in hepatocellular carcinoma through the Wnt/ β -catenin signaling [14]. The database analyses suggested that high expression of DYNLL1 indicates poor prognosis in LUAD (Fig. 1C). The UALCAN database analysis also showed significantly elevated DYNLL1 expression in LUAD (Fig. 1D). Consistent with the bioinformatics insights, we identified substantially elevated DYNLL1 levels in LUAD cells (A549, NCI-1395, and NCI-H441) versus the normal BEAS-2B cells (Fig. 1E, F). Among the LUAD cell lines, NCI-H1395 and NCI-H441 cells showed higher DYNLL1 levels were selected for following functional assays.

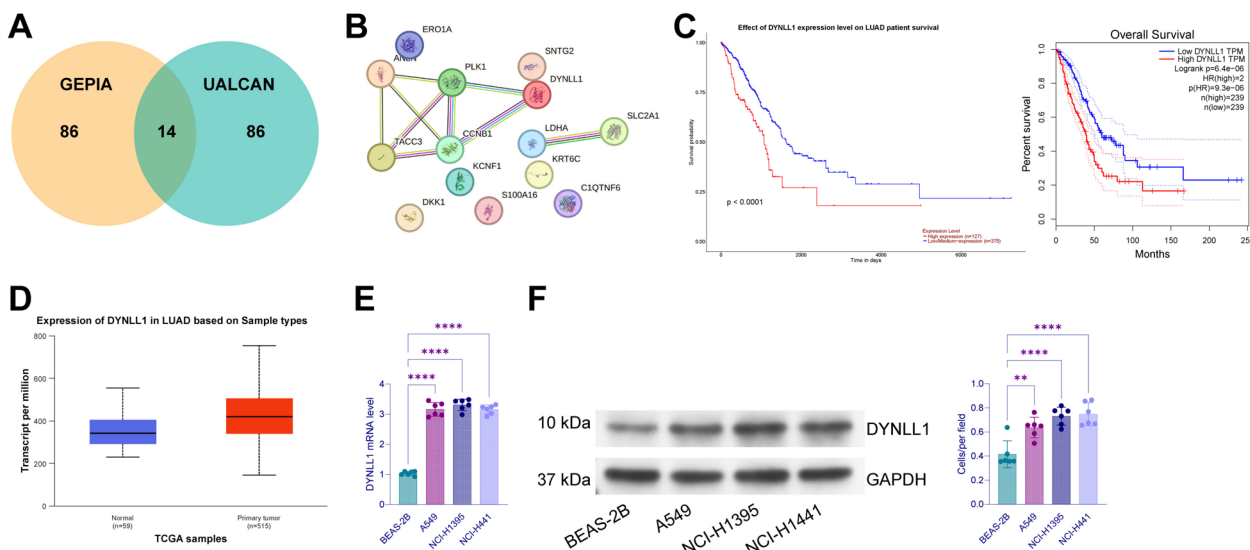


Fig. 1 DYNLL1 is abnormally upregulated in LUAD. **A** Venn diagram illustrating the intersection of prognostic markers identified in the GEPIA and UALCAN databases. **B** Protein–protein interaction (PPI) network of the intersecting genes from **(A)** generated using the STRING database. **C** Correlation of DYNLL1 expression with patient prognosis in LUAD, analyzed using the UALCAN (*left*) and GEPIA (*right*) databases, with survival analysis performed via Kaplan–Meier plots and *p*-values determined by the log-rank test. **D** Differential expression analysis of DYNLL1 in LUAD and normal lung tissues using data from the UALCAN database. **E, F** mRNA (**E**) and protein (**F**) expression levels of DYNLL1 in normal lung epithelial cells (BEAS-2B) and LUAD cell lines (A549, NCI-H1395, and NCI-H441) detected by qPCR and western blot (WB). The exact number of cells used for qPCR and WB are provided in the methods section. Each *dot* corresponds to one independent experiment. Differences were analyzed by one-way ANOVA (**E, F**). ***p* < 0.01, *****p* < 0.0001

Silencing of DYNLL1 reduces malignant phenotype of LUAD cells and blocks cell cycle progression

Three KD-DYNLL1 plasmids were administered into NCI-H1395 and NCI-H441 cells. The best-performing KD-DYNLL1 2# was selected for subsequent experiments (Fig. 2A). The DYNLL1 knockdown impaired cell proliferation activity and reduced colony formation ability (Fig. 2B). Immunofluorescence analysis exhibited a decrease in the expression of the proliferation-related factor Ki67 (Fig. 2C). Flow cytometry revealed a notable increase in cell apoptosis after DYNLL1 knockdown (Fig. 2D). This condition also hindered cell migration and invasion (Fig. 2E, F). Moreover, the DYNLL1 knockdown resulted in G0/G1 cell cycle arrest (Fig. 2G). WB analysis revealed a reduction in Cyclin D1 expression while an upregulation in p21 expression in cells with DYNLL1 knockdown. Furthermore, the β-catenin levels in cells were reduced by KD-DYNLL1 as well (Fig. 2H).

KY19382 restores cell cycle progression in LUAD cells inhibited under DYNLL1 knockdown

To analyze if Wnt/β-catenin is implicated in DYNLL1-mediated events, NCI-H1395 and NCI-H441 transfected with KD-DYNLL1 were additionally treated with KY19382, a potent Wnt/β-catenin agonists that activates this signaling by inhibiting the CXXC5-DVL interaction and GSK3β activity. The KY19382 treatment

significantly restored proliferation activity of the LUAD cell lines (Fig. 3A, B), reduced cell apoptosis (Fig. 3C), and reduced the cell cycle arrest (Fig. 3D). This procedure also increased Cyclin D1 expression while reducing p21 expression levels (Fig. 3E). Furthermore, the SABG showed that DYNLL1 silencing induced cell senescence, which was negated after β-catenin activation (Fig. 3F).

TEAD4 mediates transcriptional activation of DYNLL1 in LUAD

To figure out the causes of heightened DYNLL1 expression in LUAD, genes significantly correlated with DYNLL1 expression were queried from the UALCAN database (heatmap shows the top 25 genes) (Fig. 4A). Furthermore, potential transcription factors of DYNLL1 were downloaded from the hTFtarget database (<http://bioinfo.life.hust.edu.cn/hTFtarget/#/>). The intersection of the two datasets revealed 6 common factors (Fig. 4B): FOXM1, TEAD4, HDAC2, E2F7, NFYB, ZNF143. Among these, TEAD4 that has been reported to promote glycolysis and cell metastasis in LUAD [18, 19] caught our attention. Analysis of the UALCAN database revealed that TEAD4 was correlated with DYNLL1 expression (PearsonCC=0.38) (Fig. 4C). The GEPIA data also showed a positive correlation between these two (Fig. 4D). Kaplan–Meier Plotter suggested that high TEAD4 expression linking to unfavorable prognosis in

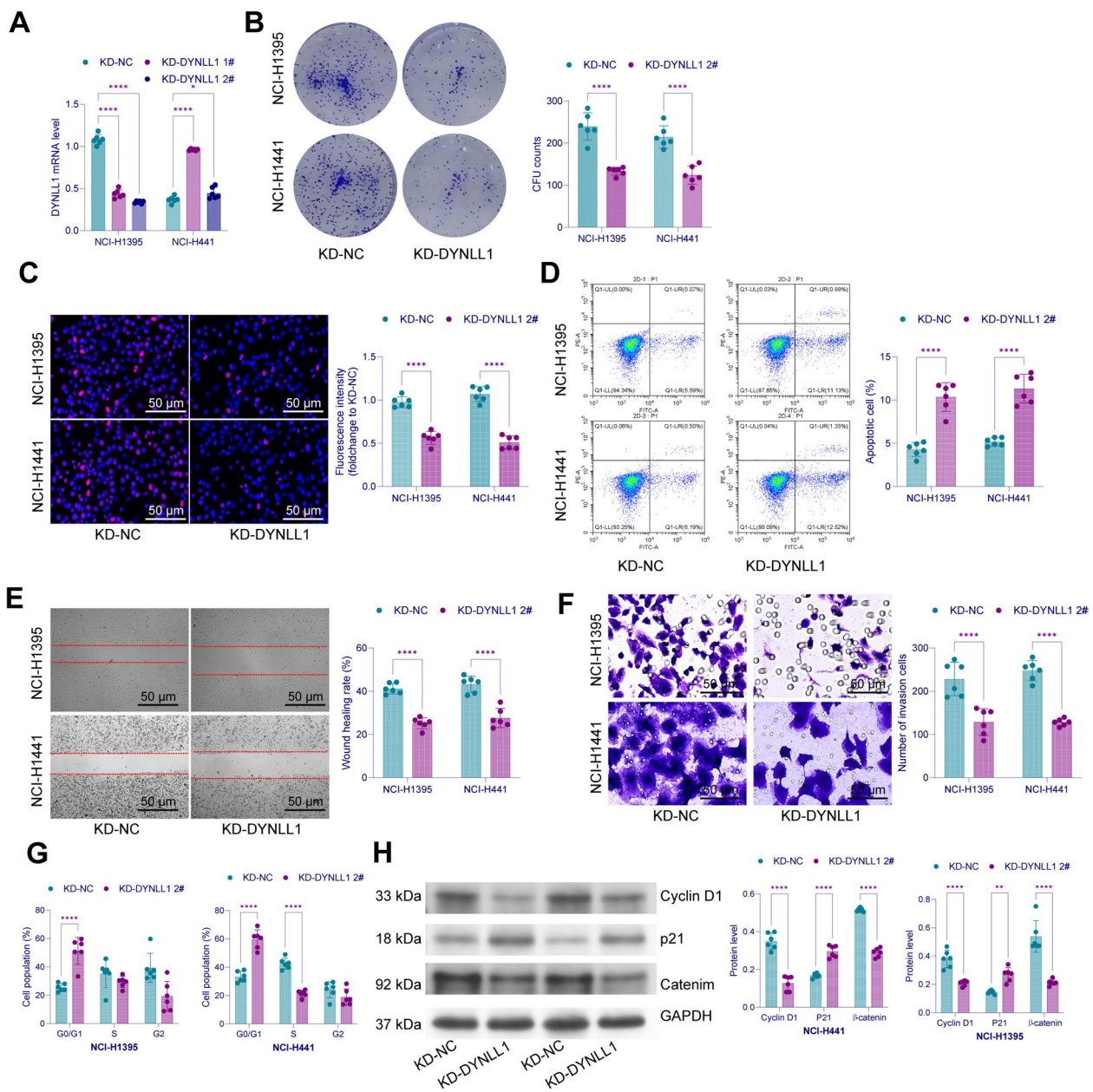


Fig. 2 Silencing of DYNLL1 reduces malignant phenotype of LUAD cells and blocks cell cycle progression. Three KD-DYNLL1 plasmids (KD-DYNLL1 1#, 2#, 3#) were transfected into NCI-H1395 and NCI-H441 cells using lentiviral vectors. **A** DYNLL1 mRNA levels in transfected cells were measured by qPCR, with KD-DYNLL1 2# exhibiting the strongest knockdown effect, selected for subsequent experiments. **B** Colony formation assay to evaluate the colony-forming ability of KD-DYNLL1-transfected cells. **C** Immunofluorescence staining for Ki67 to assess cell proliferation potential. **D** Flow cytometry analysis of cell apoptosis. **E** Wound healing assays to evaluate cell migration. **F** Transwell assay to assess cell invasion. **G** Flow cytometry analysis of cell cycle distribution. **H** Western blot analysis of protein expression levels of Cyclin D1, p21, and β-catenin in transfected cells. Each dot corresponds to one independent experiment. Differences were analyzed by two-way ANOVA (**A-H**) * $p < 0.05$, ** $p < 0.01$, **** $p < 0.0001$

LUAD patients (Fig. 4E). ChIP-seq analysis revealed significant enrichment of TEAD4 at the DYNLL1 promoter, indicating that TEAD4 possibly mediates DYNLL1 activation in LUAD, accelerating cancer progression through the cell cycle regulation.

Indeed, increased TEAD4 expression was detected in LUAD cells versus normal BEAS-2B cells (Fig. 4F). TEAD4 knockdown was then induced in LUAD cells using three plasmids, with the most effective KD-TEAD4 3# selected for subsequent use (Fig. 4G). Importantly, the

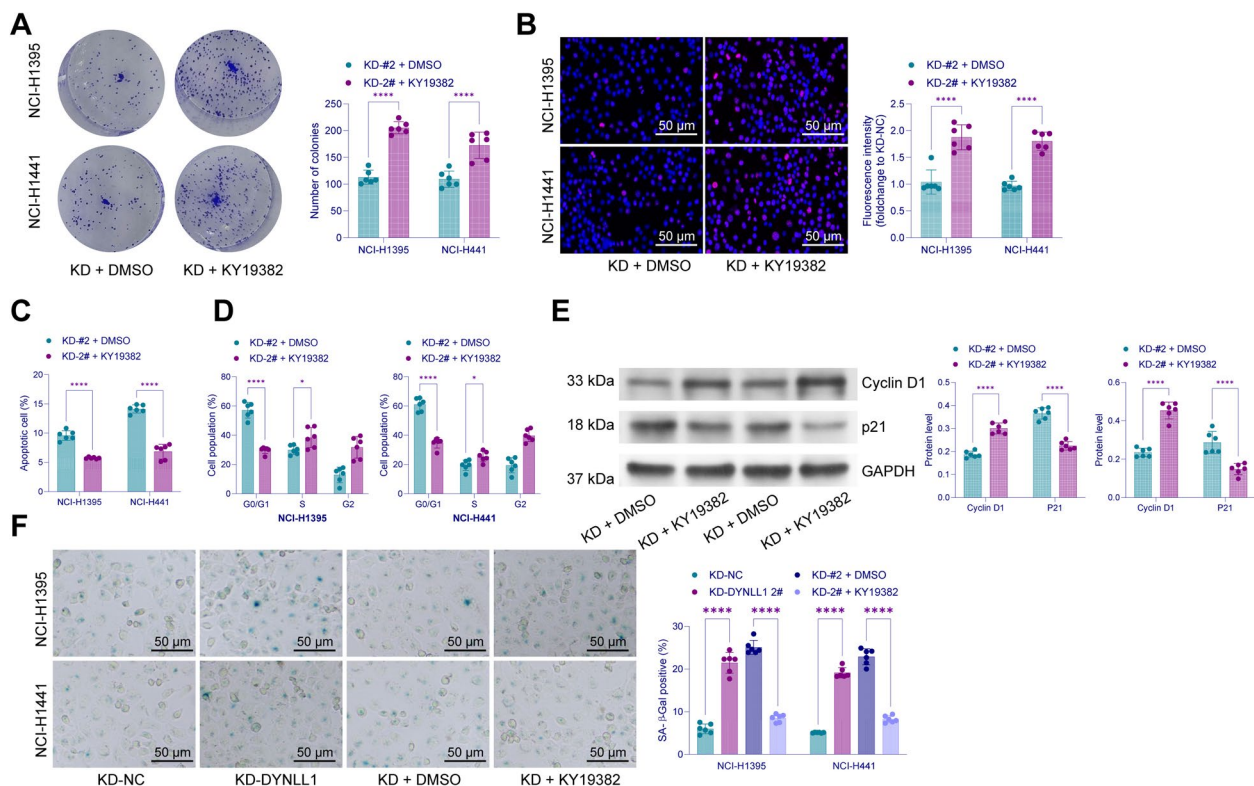


Fig. 3 KY19382 restores cell cycle progression in LUAD cells inhibited under DYNLL1 knockdown. NCI-H1395 and NCI-H441 cells transfected with KD-DYNLL1 were additionally treated with KY19382. **A** Colony formation assays to evaluate the colony-forming ability of treated cells. **B** Immunofluorescence staining for Ki67 to assess cell proliferation. **C** Flow cytometry analysis for cell apoptosis. **D** Flow cytometry analysis of cell cycle distribution. **E** Western blot analysis of protein expression levels of Cyclin D1 and p21. **F** SA-β-Gal (SABG) staining for the detection of cell senescence. Each dot corresponds to one independent expression experiment. Differences were analyzed by two-way ANOVA (**A–F**). * $p < 0.05$, **** $p < 0.0001$

TEAD4 knockdown substantially decreased DYNLL1 expression (Fig. 4H). This procedure also reduced luciferase activity of the reporter containing DYNLL1 promoter (Fig. 4I). ChIP-qPCR analysis showed significant enrichment of TEAD4 at the DYNLL1 promoter (Fig. 4J).

DYNLL1 overexpression activates Wnt/β-catenin and rescues malignant properties of LUAD cells suppressed by TEAD4 knockdown

NCI-1395 and NCI-H441 cells transfected with KD-TEAD4 were additionally administered OE-DYNLL1, which effectively rescued the DYNLL1 mRNA expression (Fig. 5A). Functional assessments revealed that TEAD4 knockdown inhibited LUAD cell proliferation activity (Fig. 5B, C) while promoting cell apoptosis (Fig. 5D). Meanwhile, the cell cycle arrest (Fig. 5E) and cell senescence (Fig. 5F) were reduced by the TEAD4 knockdown, accompanied by reduced Cyclin D1 levels and increased p21 levels (Fig. 5G). These trends were reversed by the additional DYNLL1 overexpression in LUAD cells (Fig. 5B–G). Moreover, the β-catenin levels in cells were

reduced by TEAD4 knockdown but increased after DYNLL1 overexpression.

TEAD4 and DYNLL1 affects tumorigenesis of LA795 cells in mice

To validate the functions of the TEAD4-DYNLL1 cascade in LUAD progression, mouse LUAD cells (LA795) stably transfected with KD-TEAD4 and OE-DYNLL1 were implanted into BALB/c mice to induce allograft tumors. Tumor growth analysis showed that TEAD4 knockdown inhibited tumor growth and obstructed volume increase, but overexpression of DYNLL1 accelerated tumor growth and increased tumor weight, reversing the effect of TEAD4 knockdown (Fig. 6A, B). After isolating the tumors, WB analysis demonstrated that β-catenin, TEAD4, and DYNLL1 levels within tumors were significantly reduced upon TEAD4 knockdown, while β-catenin and DYNLL1 levels were restored following DYNLL1 overexpression (Fig. 6C). IHC revealed that the positive staining of Ki67 and PCNA in tumor tissues was reduced after TEAD4 knockdown, phenomena reversed by DYNLL1

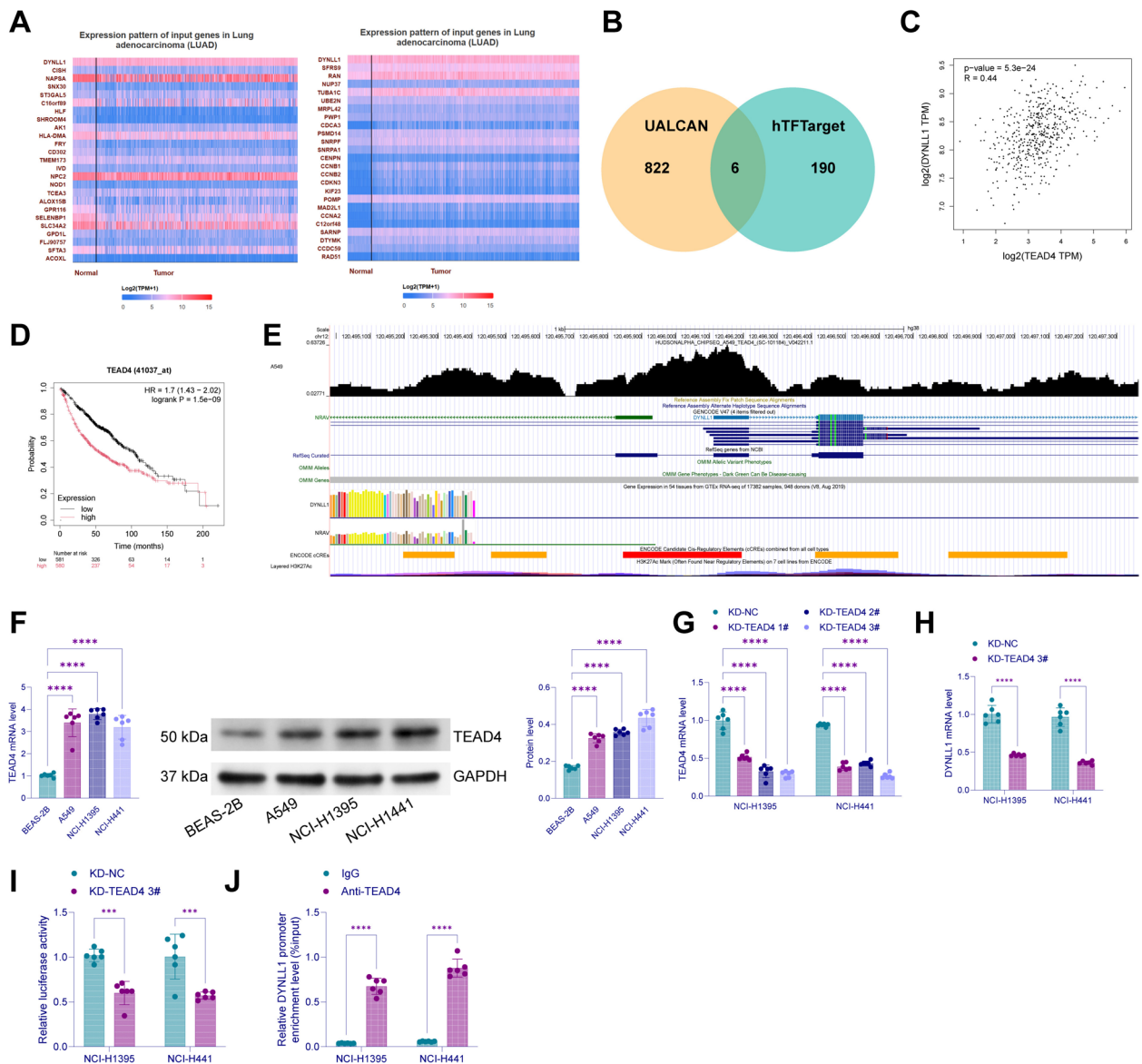


Fig. 4 TEAD4 mediates transcriptional activation of DYNLL1 in LUAD. **A** Heatmap of genes correlated with DYNLL1 expression in LUAD, obtained from the UALCAN database. **B** Intersection of genes related to DYNLL1 expression and potential transcription factors predicted to target DYNLL1, identified using the hTFtarget database. **C** Correlation between TEAD4 expression and DYNLL1 in LUAD, analyzed using the GEPIA database. **D** Kaplan–Meier plot analyzing the correlation between TEAD4 expression and patient prognosis in LUAD. **E** ChIP-seq analysis of TEAD4 binding peaks at the DYNLL1 promoter region. **F** TEAD4 expression in normal lung epithelial cells (BEAS-2B) and human LUAD cell lines (A549, NCI-H1395, and NCI-H441) measured by qPCR and Western blot (WB). Three KD-TEAD4 plasmids (KD-TEAD4 1#, 2#, 3#) were transfected into NCI-H1395 and NCI-H441 cells using lentiviral vectors. **G** qPCR analysis of TEAD4 mRNA expression in transfected cells. KD-TEAD4 3# exhibited the strongest knockdown effect and was selected for subsequent experiments. **H** qPCR analysis of DYNLL1 expression after knockdown of TEAD4 in LUAD cells. **I** Dual-luciferase reporter assay to evaluate changes in luciferase activity following TEAD4 knockdown in LUAD cells. **J** ChIP-qPCR analysis of TEAD4 enrichment at the DYNLL1 promoter in LUAD cells. Differences were analyzed by one-way (**F**) or two-way (**G–J**) ANOVA. Each dot corresponds to one independent experiment. *** $p < 0.001$, **** $p < 0.0001$

overexpression again (Fig. 6D). Mirroring the changes in vitro, TEAD4 knockdown reduced Cyclin D1 expression while enhancing p21 levels in tumors, effects counteracted by DYNLL1 restoration (Fig. 6E). Finally,

TUNEL assays showed that the cell apoptosis in the tumor tissues was induced by TEAD4 reduced alleviated after DYNLL1 overexpression (Fig. 6F). These observations support the TEAD4-DYNLL1 axis as an oncogenic cascade in LUAD progression.

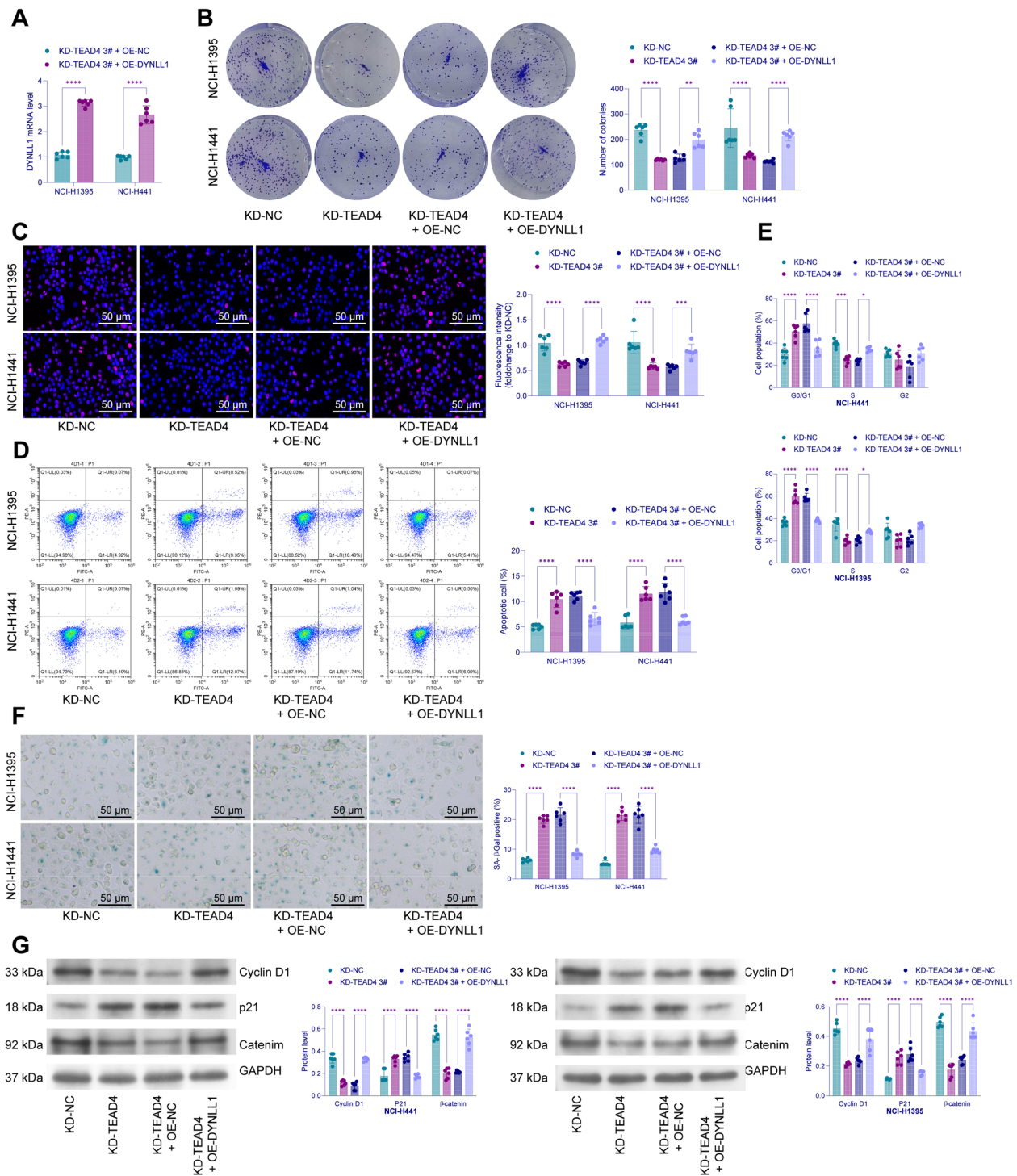


Fig. 5 DYNLL1 overexpression activates the Wnt/ β -catenin pathway and rescues malignant properties of LUAD cells suppressed by TEAD4 knockdown. NCI-1395 and NCI-H441 cells transfected with KD-TEAD4 were additionally administered OE-DYNLL1. **A** DYNLL1 mRNA expression in cells measured by qPCR analysis. **B** Colony formation assays to evaluate the colony-forming ability of treated cells. **C** Immunofluorescence staining for Ki67 to assess cell proliferation. **D** Flow cytometry analysis of cell apoptosis. **E** Flow cytometry analysis of cell cycle distribution. **F** SA- β -Gal (SABG) staining to analyze cell senescence. **G** Western blot (WB) analysis of Cyclin D1 and p21 protein levels. Each dot corresponds to one independent experiment. Differences were analyzed by two-way ANOVA (**A-G**). * $p < 0.05$, ** $p < 0.01$, *** $p < 0.001$, **** $p < 0.0001$

Discussion

This study explores the role of TEAD4 in regulating DYNLL1 transcription, which accelerates cell cycle progression and enhances the malignant characteristics of LUAD cells, potentially via the Wnt/ β -catenin pathway (Fig. 7). The findings supporting this conclusion are as follows: (i) DYNLL1 expression is elevated in LUAD cells, and its silencing leads to G0/G1 phase cell cycle arrest, reduced cell proliferation, and impaired cell migration in vitro; (ii) knocking down DYNLL1 results in decreased β -catenin protein levels in LUAD cells; (iii) treatment with the Wnt agonist KY19382 rescues the malignant phenotype in DYNLL1-silenced LUAD cells; (iv) TEAD4 is upregulated in LUAD cells, binding directly to the DYNLL1 promoter to enhance its transcription; (v) knocking down TEAD4 similarly reduces β -catenin levels, arrests the cell cycle, and diminishes the malignancy of both human and mouse LUAD cells.

Researchers are actively investigating reliable prognostic biomarkers and therapeutic targets in cancer to improve cancer treatment [20–22]. In this paper, we generated a key interaction network based on prognostic markers from GEPIA and UALCAN datasets. This network includes several central proteins, such as ANLN, PLK1, DYNLL1, CCNB1, and TACC3. Among these, the roles of ANLN [23, 24], PLK1 [25, 26], TACC3 [27], and CCNB1 [28, 29] in LUAD have been investigated. Therefore, DYNLL1 was selected for subsequent research. Our initial finding confirmed that DYNLL1 is overexpressed in LUAD cells, which aligns with bioinformatics data. DYNLL1, a dynein light chain protein, plays a critical role in DNA double-strand break repair by regulating DNA end resection [30, 31]. A loss of DYNLL1 has been linked to chemoresistance in ovarian cancer [32, 33]. However, its role in cancer appears context-dependent, as it has been associated with tumorigenesis in B-cell lymphoma [34] and cell survival in esophageal cancer [35]. In our study, silencing DYNLL1 in LUAD cells led to reduced cell proliferation, migration, and G0/G1 phase cell cycle arrest, while increasing apoptosis. These changes were accompanied by a reduction in Cyclin D1 and an upregulation in p21. These observations are in line with studies in hepatocellular carcinoma [13], where DYNLL1 suppression also affected cell progression and β -catenin

levels [14]. The Wnt/ β -catenin signaling, well characterized for driving cancer cell malignancy, including cell cycle progression [36, 37], was found to be involved in the oncogenic effects of DYNLL1, as treatment with the Wnt agonist KY19382 reversed the suppression of the malignant phenotype caused by DYNLL1 knockdown in LUAD cells.

The regulation of DYNLL1 expression in cancer may be influenced by specific transcription factors [34]. Bioinformatics analysis suggested TEAD4 as a potential transcription factor for DYNLL1. TEAD4 is known to possess a TEA DNA-binding domain that interacts with gene promoters, along with a binding domain for YAP/TAZ, which associates with coactivators [16]. Using luciferase and ChIP assays, we confirmed that TEAD4 binds directly to the DYNLL1 promoter. TEAD4 expression is often upregulated in various cancers, where it promotes tumorigenesis by enhancing cancer stemness, metastasis, and drug resistance [38]. While its role in cell cycle regulation is not well understood, TEAD4 has been shown to facilitate glycolysis and metastasis in LUAD [18, 19]. Consistent with previous findings, we observed elevated TEAD4 expression in LUAD cells, which likely contributes to the aberrant upregulation of DYNLL1 in this context. In gastric cancer, TEAD4 has been shown to activate the transcription of PRIM1 and other cell cycle regulators, such as Cdc25, Cyclin B, and Cdc2 [39]. Our study extended these observations by showing that silencing TEAD4 in LUAD cells led to reduced β -catenin levels, decreased DYNLL1 expression, and triggered cell cycle arrest, senescence, and apoptosis. In animal models, silencing TEAD4 in LUAD cells resulted in reduced tumorigenicity in mice, an effect that could be reversed by restoring DYNLL1 expression.

Nevertheless, there are several shortcomings that need to be acknowledged. First, while TEAD4 has been identified as an upstream transcription factor regulating DYNLL1 transcription and contributing to LUAD progression in these experiments, other potential causative factors may not have been fully explored. Second, gain-of-function experiments involving DYNLL1 or TEAD4 were not thoroughly performed in this study. Additionally, the lack of clinical samples and ethical constraints prevented us from providing clinical data, which may

(See figure on next page.)

Fig. 6 TEAD4 and DYNLL1 affects tumorigenesis of LA795 cells in mice. Mouse LUAD cells (LA795; 5×10^6 cells per mouse) stably transfected with KD-TEAD4 and OE-DYNLL1 were implanted into BALB/c mice to induce allograft tumors. **A** Tumor volume measured over a 5-week period. **B** Representative images of tumors and tumor weight after 5 weeks of growth. **C** Western blot (WB) analysis for the expression of β -catenin, TEAD4, and DYNLL1 in tumor tissues. **D** Immunohistochemistry (IHC) for the positive staining of proliferation markers Ki67 and PCNA in tumor tissues. **E** IHC for the positive staining of Cyclin D1 and p21 levels in tumor tissues. **F** TUNEL assays to detect cell apoptosis within the tumor tissues. Differences were analyzed by two-way ANOVA (**A–F**). Each group contained six mice. * $p < 0.05$, ** $p < 0.01$, *** $p < 0.001$, **** $p < 0.0001$

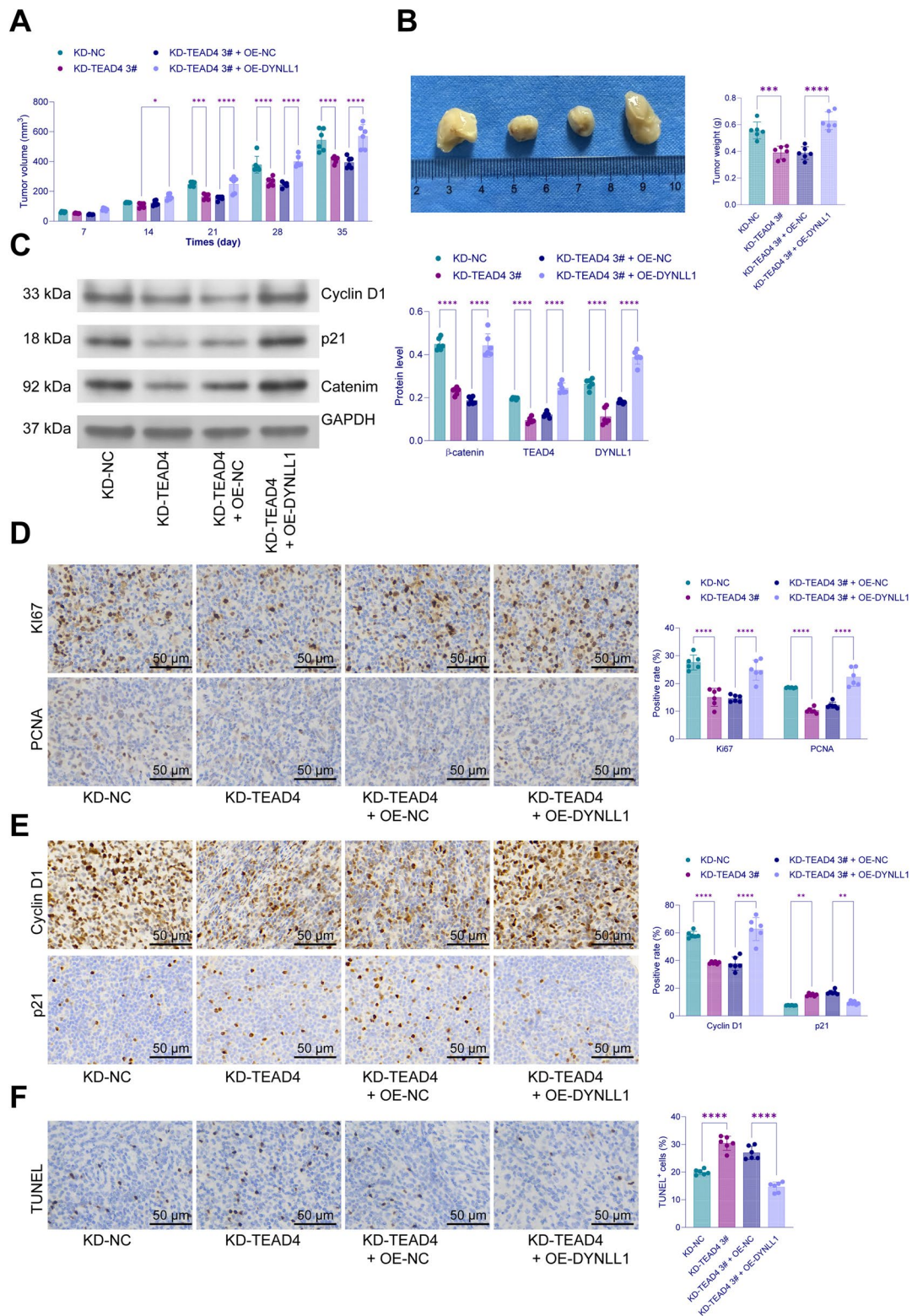


Fig. 6 (See legend on previous page.)

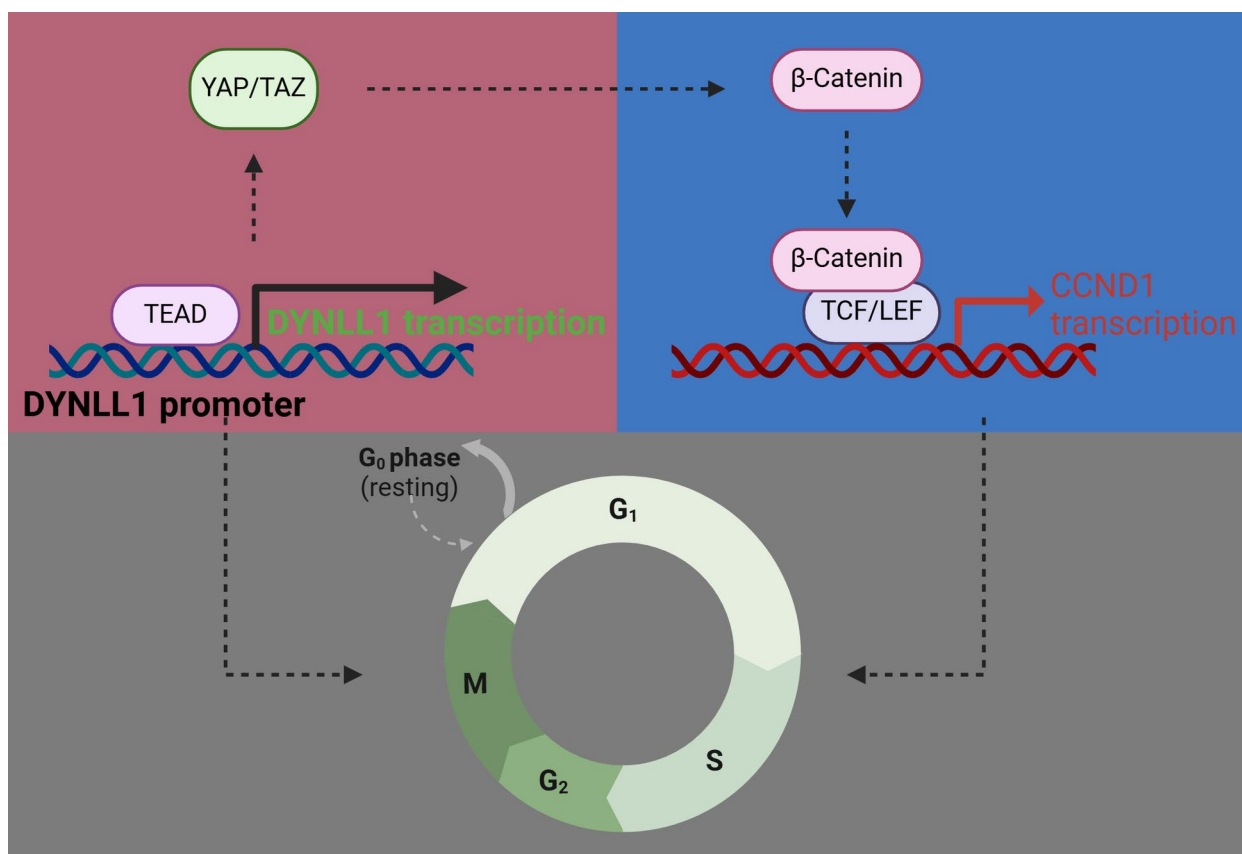


Fig. 7 Graphic Abstract. TEAD4 regulates DYNLL1 transcription to activate the Wnt/ β -catenin signaling, thus promoting cell cycle progression and the malignant properties of LUAD cells

have limited the translational value of this study. We aim to address these issues and offer a more comprehensive understanding in future investigations.

Conclusion

In conclusion, our study proves that TEAD4 regulates DYNLL1 transcription to activate the Wnt/ β -catenin signaling, thus promoting cell cycle progression and the malignant properties of LUAD cells. The TEAD4/DYNLL1 axis may thus represent a new therapeutic target for LUAD treatment. However, the lack of clinical data limits the translational implications of this study, and further research is needed to validate the prognostic value of TEAD4 and DYNLL1 in LUAD. Future studies will aim to fill this gap and deepen our understanding of these molecular interactions.

Supplementary Information

The online version contains supplementary material available at <https://doi.org/10.1186/s40001-025-02500-y>.

Additional file 1.

Acknowledgements

Not applicable.

Author contributions

DPL, AW and DYH contributed to the idea of the study and design of the research. XW, MKS and YBL performed the experiments and contributed to the collection of data, the analysis of statistics and manuscript preparation. XFC and DPL drafted and modified the manuscript. The manuscript was read and approved by all authors.

Funding

This study was supported by the special project of clinical research of Shanghai Health Commission (No.202040454) and the Young Scientists Fund of the National Natural Science Foundation of China (No. 82303497).

Availability of data and materials

The datasets generated during and/or analyzed during the current study are available from the corresponding author on reasonable request.

Declarations

Ethics approval and consent to participate

All animals used in guidelines approved by the Institutional Animal Care and Use Committee of the First Affiliated Hospital of Soochow University (approval no. 2024-HSYY-551) in strict adherence to the Guide for the Care and Use of

Laboratory Animals (NIH, Bethesda, MD, USA). The report of animal experiments is following the ARRIVE guidelines.

Consent for publication

Not applicable.

Competing interests

The authors declare no competing interests.

Received: 23 January 2025 Accepted: 24 March 2025

Published online: 01 April 2025

References

- Herbst RS, Morgensztern D, Boshoff C. The biology and management of non-small cell lung cancer. *Nature*. 2018;553(7689):446–54. <https://doi.org/10.1038/nature25183>.
- Succony L, Rassl DM, Barker AP, McCaughan FM, Rintoul RC. Adenocarcinoma spectrum lesions of the lung: detection, pathology and treatment strategies. *Cancer Treat Rev*. 2021;99: 102237. <https://doi.org/10.1016/j.ctrv.2021.102237>.
- Saito M, Shiraiishi K, Kunitoh H, Takenoshita S, Yokota J, Kohno T. Gene aberrations for precision medicine against lung adenocarcinoma. *Cancer Sci*. 2016;107(6):713–20. <https://doi.org/10.1111/cas.12941>.
- Du X, Yang B, An Q, Assaraf YG, Cao X, Xia J. Acquired resistance to third-generation EGFR-TKIs and emerging next-generation EGFR inhibitors. *Innovation (Camb)*. 2021;2(2): 100103. <https://doi.org/10.1016/j.xinn.2021.100103>.
- Meng X, Zhu X, Ji J, Zhong H, Li X, Zhao H, et al. Erdafitinib inhibits tumorigenesis of human lung adenocarcinoma A549 by inducing S-phase cell-cycle arrest as a CDK2 inhibitor. *Molecules*. 2022;27(19):6733. <https://doi.org/10.3390/molecules27196733>.
- Hirsch FR, Scagliotti GV, Mulshine JL, Kwon R, Curran WJ Jr, Wu YL, et al. Lung cancer: current therapies and new targeted treatments. *Lancet*. 2017;389(10066):299–311. [https://doi.org/10.1016/S0140-6736\(16\)30958-8](https://doi.org/10.1016/S0140-6736(16)30958-8).
- Brock MV, Hooker CM, Ota-Machida E, Han Y, Guo M, Ames S, et al. DNA methylation markers and early recurrence in stage I lung cancer. *N Engl J Med*. 2008;358(11):1118–28. <https://doi.org/10.1056/NEJMoa0706550>.
- Wang W, Yang C, Deng H. Overexpression of 15-hydroxyprostaglandin dehydrogenase inhibits A549 lung adenocarcinoma cell growth via inducing cell cycle arrest and inhibiting epithelial-mesenchymal transition. *Cancer Manag Res*. 2021;13:8887–900. <https://doi.org/10.2147/CMAR.S331222>.
- Hall J, Hall A, Pursifull N, Barbar E. Differences in dynamic structure of LC8 monomer, dimer, and dimer-peptide complexes. *Biochemistry*. 2008;47(46):11940–52. <https://doi.org/10.1021/bi801093k>.
- Rapali P, Szenes A, Radnai L, Bakos A, Pal G, Nyitray L. DYNLL/LC8: a light chain subunit of the dynein motor complex and beyond. *FEBS J*. 2011;278(17):2980–96. <https://doi.org/10.1111/j.1742-4658.2011.08254.x>.
- Jespersen N, Barbar E. Emerging features of linear motif-binding hub proteins. *Trends Biochem Sci*. 2020;45(5):375–84. <https://doi.org/10.1016/j.tibs.2020.01.004>.
- Dunsch AK, Hammond D, Lloyd J, Schermelleh L, Gruneberg U, Barr FA. Dynein light chain 1 and a spindle-associated adaptor promote dynein asymmetry and spindle orientation. *J Cell Biol*. 2012;198(6):1039–54. <https://doi.org/10.1083/jcb.201202112>.
- Liu Y, Li Z, Zhang J, Liu W, Guan S, Zhan Y, et al. DYNLL1 accelerates cell cycle via ILF2/CDK4 axis to promote hepatocellular carcinoma development and palbociclib sensitivity. *Br J Cancer*. 2024;131(2):243–57. <https://doi.org/10.1038/s41416-024-02719-2>.
- Shen Y, Chen J, Zhou Z, Wu J, Hu X, Xu Y, et al. Matrix stiffness-related extracellular matrix signatures and the DYNLL1 protein promote hepatocellular carcinoma progression through the Wnt/beta-catenin pathway. *BMC Cancer*. 2024;24(1):1211. <https://doi.org/10.1186/s12885-024-12973-5>.
- Veland IR, Awan A, Pedersen LB, Yoder BK, Christensen ST. Primary cilia and signaling pathways in mammalian development, health and disease. *Nephron Physiol*. 2009;111(3):p39-53. <https://doi.org/10.1159/000208212>.
- Chen M, Huang B, Zhu L, Chen K, Liu M, Zhong C. Structural and functional overview of TEAD4 in cancer biology. *Onco Targets Ther*. 2020;13:9865–74. <https://doi.org/10.2147/OTT.S266649>.
- Shao M, Wang L, Zhang Q, Wang T, Wang S. STMN2 overexpression promotes cell proliferation and EMT in pancreatic cancer mediated by WNT/beta-catenin signaling. *Cancer Gene Ther*. 2023;30(3):472–80. <https://doi.org/10.1038/s41417-022-00568-w>.
- Zhang Q, Fan H, Zou Q, Liu H, Wan B, Zhu S, et al. TEAD4 exerts prometastatic effects and is negatively regulated by miR6839-3p in lung adenocarcinoma progression. *J Cell Mol Med*. 2018;22(7):3560–71. <https://doi.org/10.1111/jcmm.13634>.
- Hu Y, Mu H, Deng Z. The transcription factor TEAD4 enhances lung adenocarcinoma progression through enhancing PKM2 mediated glycolysis. *Cell Biol Int*. 2021;45(10):2063–73. <https://doi.org/10.1002/cbin.11654>.
- Marschollek K, Brzecka A, Pokryszko-Dragan A. New biochemical, immune and molecular markers in lung cancer: diagnostic and prognostic opportunities. *Adv Clin Exp Med*. 2022;31(12):1391–411. <https://doi.org/10.17219/acem/152349>.
- Liang S, Wang H, Tian H, Xu Z, Wu M, Hua D, et al. The prognostic biological markers of immunotherapy for non-small cell lung cancer: current landscape and future perspective. *Front Immunol*. 2023;14:1249980. <https://doi.org/10.3389/fimmu.2023.1249980>.
- Meira DD, de Castro ECM, Casotti MC, Zetum ASS, Goncalves AFM, Moreira AR, et al. Prognostic factors and markers in non-small cell lung cancer: recent progress and future challenges. *Genes (Basel)*. 2023;14(10):1906. <https://doi.org/10.3390/genes14101906>.
- Sheng L, Kang Y, Chen D, Shi L. Knockdown of ANLN inhibits the progression of lung adenocarcinoma via pyroptosis activation. *Mol Med Rep*. 2023;28(3):177. <https://doi.org/10.3892/mmr.2023.13064>.
- Ting Z, Wu Z, Yang C, Li Z, Huang H, Gan J, et al. lncRNA CERS6-AS1 upregulates the expression of ANLN by sponging miR-424-5p to promote the progression and drug resistance of lung adenocarcinoma. *Noncoding RNA Res*. 2024;9(1):221–35. <https://doi.org/10.1016/j.ncrna.2023.11.013>.
- Jang HR, Shin SB, Kim CH, Won JY, Xu R, Kim DE, et al. PLK1/vimentin signaling facilitates immune escape by recruiting Smad2/3 to PD-L1 promoter in metastatic lung adenocarcinoma. *Cell Death Differ*. 2021;28(9):2745–64. <https://doi.org/10.1038/s41418-021-00781-4>.
- Chen M, Zhang S, Wang F, He J, Jiang W, Zhang L. DLGAP5 promotes lung adenocarcinoma growth via upregulating PLK1 and serves as a therapeutic target. *J Transl Med*. 2024;22(1):209. <https://doi.org/10.1186/s12967-024-04910-8>.
- Xu J, Zhu Y, Liu Q, Xu C, Wang W, Sun J, et al. Prognostic and immunotherapeutic role of TACC3 in pancancer and its impact on proliferation and docetaxel resistance in lung adenocarcinoma. *Oncology*. 2024. <https://doi.org/10.1159/000542450>.
- Xiao X, Rui B, Rui H, Ju M, Hongtao L. MEOX1 suppresses the progression of lung cancer cells by inhibiting the cell-cycle checkpoint gene CCNB1. *Environ Toxicol*. 2022;37(3):504–13. <https://doi.org/10.1002/tox.23416>.
- Wang F, Fu X, Chang M, Wei T, Lin R, Tong H, et al. The interaction of calcium-sensing receptor with KIF11 enhances cisplatin resistance in lung adenocarcinoma via BRCA1/cyclin B1 pathway. *Int J Biol Sci*. 2024;20(10):3892–910. <https://doi.org/10.7150/ijbs.92046>.
- Becker JR, Cuella-Martin R, Barazas M, Liu R, Oliveira C, Oliver AW, et al. The ASCIZ-DYNLL1 axis promotes 53BP1-dependent non-homologous end joining and PARP inhibitor sensitivity. *Nat Commun*. 2018;9(1):5406. <https://doi.org/10.1038/s41467-018-07855-x>.
- Swift ML, Zhou R, Syed A, Moreau LA, Thomas B, Tainer JA, et al. Dynamics of the DYNLL1-MRE11 complex regulate DNA end resection and recruitment of Shieldin to DSBs. *Nat Struct Mol Biol*. 2023;30(10):1456–67. <https://doi.org/10.1038/s41594-023-01074-9>.
- Berkel C, Cacan E. In silico analysis of DYNLL1 expression in ovarian cancer chemoresistance. *Cell Biol Int*. 2020;44(8):1598–605. <https://doi.org/10.1002/cbin.11352>.
- Berkel C, Cacan E. Involvement of ATMIN-DYNLL1-MRN axis in the progression and aggressiveness of serous ovarian cancer. *Biochem Biophys Res Commun*. 2021;570:74–81. <https://doi.org/10.1016/j.bbrc.2021.07.004>.

34. Wong DM, Li L, Jurado S, King A, Bamford R, Wall M, et al. The transcription factor ASCIZ and its target DYNLL1 are essential for the development and expansion of MYC-Driven B cell lymphoma. *Cell Rep.* 2016;14(6):1488–99. <https://doi.org/10.1016/j.celrep.2016.01.012>.
35. Li Q, Zhang Z, Jiang H, Hou J, Chai Y, Nan H, et al. DLEU1 promotes cell survival by preventing DYNLL1 degradation in esophageal squamous cell carcinoma. *J Transl Med.* 2022;20(1):245. <https://doi.org/10.1186/s12967-022-03449-w>.
36. Xiong J, Xing S, Dong Z, Niu L, Xu Q, Liu P, et al. STK31 regulates the proliferation and cell cycle of lung cancer cells via the Wnt/beta-catenin pathway and feedback regulation by c-myc. *Oncol Rep.* 2020;43(2):395–404. <https://doi.org/10.3892/or.2019.7441>.
37. Zhang J, Zhang X, Yang S, Bao Y, Xu D, Liu L. FOXH1 promotes lung cancer progression by activating the Wnt/beta-catenin signaling pathway. *Cancer Cell Int.* 2021;21(1):293. <https://doi.org/10.1186/s12935-021-01995-9>.
38. Hsu SC, Lin CY, Lin YY, Collins CC, Chen CL, Kung HJ. TEAD4 as an oncogene and a mitochondrial modulator. *Front Cell Dev Biol.* 2022;10:890419. <https://doi.org/10.3389/fcell.2022.890419>.
39. Guo Z, Guo L. YAP/TEAD-induced PRIM1 contributes to the progression and poor prognosis of gastric carcinoma. *Transl Oncol.* 2023;38: 101791. <https://doi.org/10.1016/j.tranon.2023.101791>.

Publisher's Note

Springer Nature remains neutral with regard to jurisdictional claims in published maps and institutional affiliations.